Internal Medicine
The Japanese Society of Internal Medicine
doi: 10.2169/internalmedicine.6381-20
Intern Med 60: 1555-1560, 2021
http://internmed.jp

【 CASE REPORT 】

Mediastinal Cystic Parathyroid Adenoma Diagnosed by Somatostatin Receptor Scintigraphy

Kenichi Yokota[1], Isao Kurihara[1], Yohji Matsusaka[2], Katsura Emoto[3], Tomoyuki Hishida[4], Takuma Oshida[1], Sakiko Kobayashi[1], Ayano Murai-Takeda[1], Kazutoshi Miyashita[1], Kohei Matsuda[4], Takahiro Nakagomi[4], Kosuke Matsuda[3] and Hiroshi Itoh[1]

Abstract:
A 71-year-old man complained of nausea and loss of appetite for eight months prior to admission. He was transported to a hospital with disorientation and diagnosed with primary hyperparathyroidism by laboratory examinations. However, ultrasonography, computed tomography, and technetium-99m labeled methoxyisobutyl isonitrile (^{99m}Tc-MIBI) with single-photon emission computed tomography did not yield definite results. In contrast, somatostatin receptor scintigraphy successfully identified the lesion responsible for the oversecretion of parathyroid hormone within the middle mediastinum. The tumor was successfully resected by surgery, and a histopathological analysis confirmed the parathyroid adenoma nature of the tumor.

Key words: ^{111}In-pentetreotide scintigraphy, ectopic parathyroid adenoma, parathyroid hormone, primary hyperparathyroidism, somatostatin receptor scintigraphy

(Intern Med 60: 1555-1560, 2021)
(DOI: 10.2169/internalmedicine.6381-20)

Introduction

Primary hyperparathyroidism (PHPT) is an endocrine disorder that causes hypercalcemia due to the excessive secretion of parathyroid hormone (PTH). The identification and resection of the PHPT-responsible lesion is essential for achieving an effective cure; therefore, imaging studies are a critical diagnostic step.

Ultrasonography (US), computed tomography (CT), magnetic resonance imaging (MRI), and technetium-99m labeled methoxyisobutyl isonitrile (^{99m}Tc-MIBI) scintigraphy with single-photon emission computed tomography (SPECT) are established preoperative visualization techniques employed for lesion localization. However, such noninvasive imaging approaches yield nonlocalizing results in 12% to 18% of patients with PHPT (1-3). There have been only few case reports of PHPT in which somatostatin receptor scintigraphy (SRS) was used to identify cervical parathyroid adenomas (4-6). However, the superiority and benefit of SRS over ^{99m}Tc-MIBI scintigraphy remain unclear.

We herein report a case of ^{99m}Tc-MIBI-negative cystic parathyroid adenoma within the mediastinum diagnosed by SRS, further demonstrating the usefulness of SRS for the localization PHPT-related lesions.

Case Report

A 71-year-old man reported an 8-month history of nausea and loss of appetite with a weight loss of 10 kg prior to admission. In early August 2019, he presented to the emergency department of another hospital with disorientation. Biochemical investigations revealed severe hypercalcemia [albumin-corrected calcium (Ca): 16.8 mg/dL]. For the further examination and medication, the patient was referred to our hospital.

An assessment of his clinical history revealed that he had had tuberculosis by five years old. He had a 51-pack/year

[1]Department of Internal Medicine, Keio University School of Medicine, Japan, [2]Department of Nuclear Medicine, Saitama Medical University International Medical Center, Japan, [3]Department of Pathology, Keio University School of Medicine, Japan and [4]Division of Thoracic Surgery, Department of Surgery, Keio University School of Medicine, Japan
Received: September 24, 2020; Accepted: October 21, 2020; Advance Publication by J-STAGE: December 7, 2020
Correspondence to Dr. Kenichi Yokota, kyokota@keio.jp

Table 1. The Patient's Laboratory Findings.

Test	Result	Normal range
Albumin	3.3 g/dL	3.9-4.9 g/dL
UN	44.1 mg/dL	8.0-20.0 mg/dL
Cr	1.19 mg/dL	0.60-1.10 mg/dL
Ca	16.1 mg/dL	8.8-10.2 mg/dL
IP	2.0 mg/dL	2.5-4.5 mg/dL
Intact PTH	531 pg/mL	10-65 pg/mL
PTHrP	<1.0 pmoL/L	<1.1 pmoL/L
25(OH)VitD	10.3 ng/mL	>20 ng/mL
$1,25(OH)_2$VitD	86.0 pg/mL	20-60 pg/mL
FECa	1.49 %	2-4 %
TmP/GFR	1.5 mg/dL	2.3-4.3 mg/dL
%TRP	65.3 %	80-94 %

%TRP: percentage of tubular reabsorption of phosphate, Ca: calcium, Cr: creatinine, FECa: urine fractional excretion of calcium, IP: inorganic phosphorus, PTH: parathyroid hormone, PTHrP: parathyroid hormone-related protein, TmP/GFR: tubular maximum reabsorption of phosphorus per glomerular filtration rate, UN: urea nitrogen, VitD: vitamin D

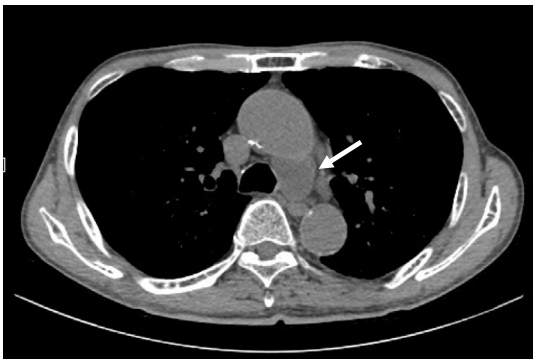

Figure 1. Computed tomography (CT) showed a cyst-like lesion in the left lower paratracheal lesion of the middle mediastinum (arrow).

smoking history and drank half a bottle of wine every day. He had no family history of hypercalcemia or endocrine neoplasm. He denied taking any medications, including over-the-counter medications.

On a neurological examination, he showed mild disorientation, which improved with subsequent treatment. On a physical examination, he had no palpable neck mass and no bone or joint pain. His laboratory data on admission (Table 1) revealed hypercalcemia, hypophosphatemia, increased PTH, suppressed parathyroid hormone-related protein (PTHrP), decreased TmP/GFR, and 24-h urine fractional excretion of calcium (FECa) >1%. His bone density was markedly reduced in both the lumbar spine and femoral neck (Table 2). Based on these findings, the patient was diagnosed with PHPT.

The administration of isotonic saline, furosemide, cinacalcet, and zoledronic acid (3 mg) improved the Ca levels, but mild hypercalcemia persisted. To identify the PHPT-responsible lesion, cervical ultrasonography (US) was performed, but no tumors were detected. CT revealed a 3-cm cyst-like lesion in the left lower paratracheal lesion of the middle mediastinum (Fig. 1) and a bone tumor-like lesion in the proximal part of the left femur (Fig. 2); the latter lesion showed a low intensity on both T1- and T2-weighted MRI, suggestive of a brown tumor (Fig. 3). Furthermore, ^{99m}Tc-MIBI scintigraphy with SPECT/CT showed no recognizable accumulation in the cervical and thoracic areas, including in the mediastinal cystic tumor (Fig. 4).

Table 2. Bone Mineral Density Results.

	BMD	T-score	Z-score	YAM
Lumbar spine	0.721 g/cm^2	-2.6	-1.8	63%
Femoral neck	0.510 g/cm^2	-4.0	-2.4	58%

BMD: bone mineral density, YAM: young adult mean

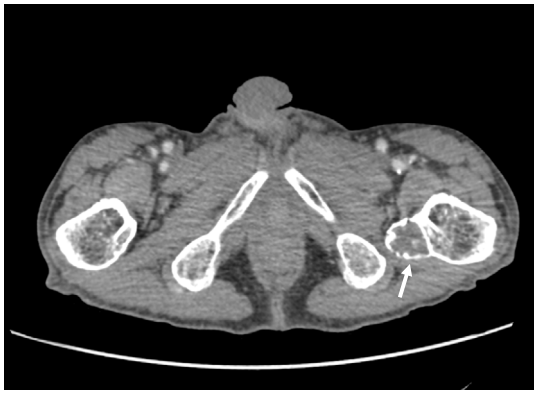

Figure 2. Computed tomography (CT) showed a bone tumor-like lesion in the proximal part of the left femur (arrow).

Given that some parathyroid adenomas are positive on SRS (4-6), we next performed SRS with SPECT/CT to identify the PHPT-responsible lesion. As shown in Fig. 5, a delayed scan (24 hours after injection) of SRS with ^{111}In-pentetreotide (Octreoscan; FUJIFILM Toyama Chemical, Tokyo, Japan) revealed the significant uptake of ^{111}In-pentetreotide in the left wall of the mediastinal cystic lesion.

Tumor resection was performed via left posterolateral mini-thoracotomy with thoracoscopic assistance, which resulted in improved values of intact PTH, Ca, and inorganic phosphorus (IP) from 570, 12.1, and 1.7 mg/dL before the surgery to 43, 9.3, and 2.3 mg/dL after the surgery, respectively. The left recurrent nerve had adhered to the tumor but was preserved by careful dissection. Although he experienced temporary mild hoarseness, he was discharged from the hospital with a generally good postoperative course.

The resected tumor was a 3-cm cystic tumor with a 1-cm solid inner part. A postoperative pathological assessment revealed that, in the wall of the cyst, parathyroid chief cell-like cells with slightly enlarged nuclei had grown in a solid nest pattern (Fig. 6). An immunohistochemical analysis further showed that these cells were positive for PTH, chromogranin A, and cytokeratin AE1/AE3 but negative for CD56

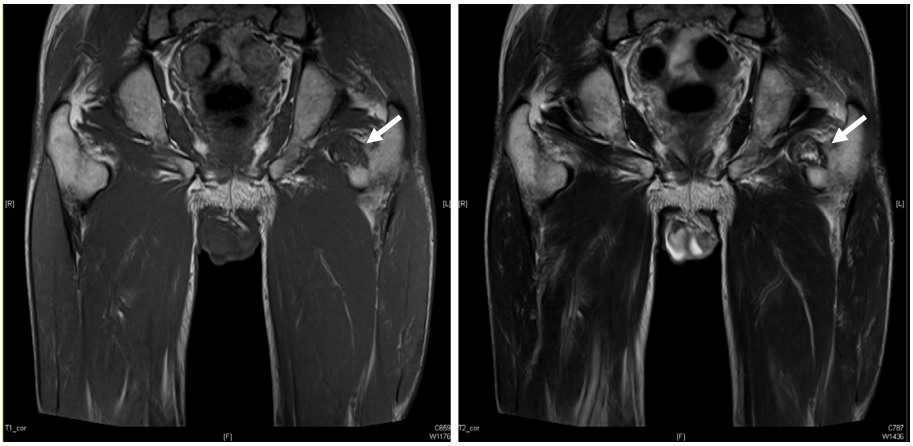

Figure 3. **Magnetic resonance imaging (MRI) of the tumor on the left femur showed a low intensity on T1- and T2-weighted scans (arrow).**

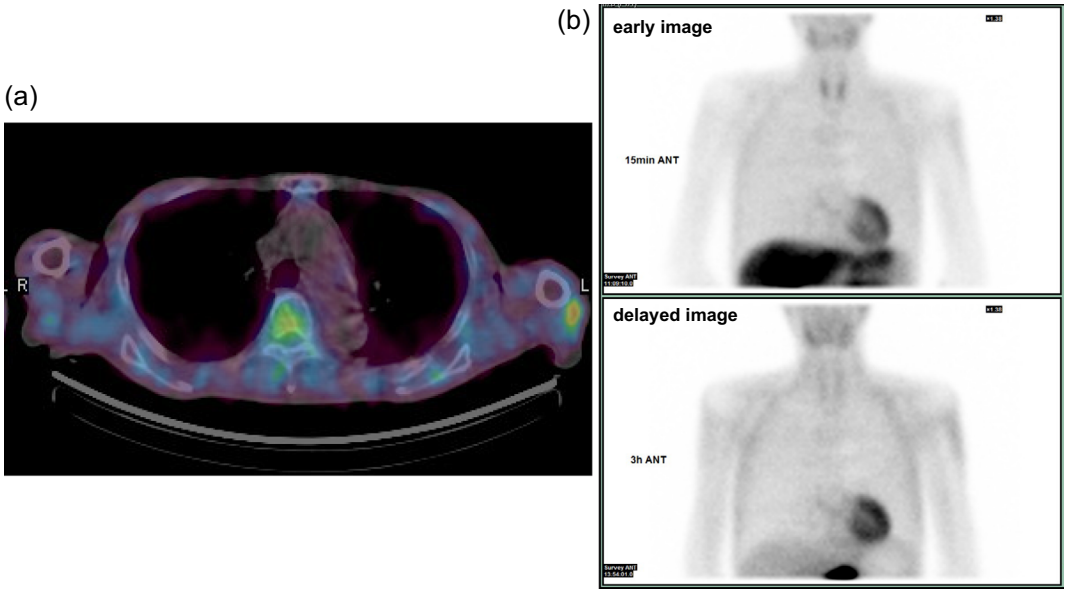

Figure 4. **^{99m}Tc-MIBI scintigraphy did not show any uptake. (a) Single-photon emission computed tomography (SPECT). (b) Planar Image.**

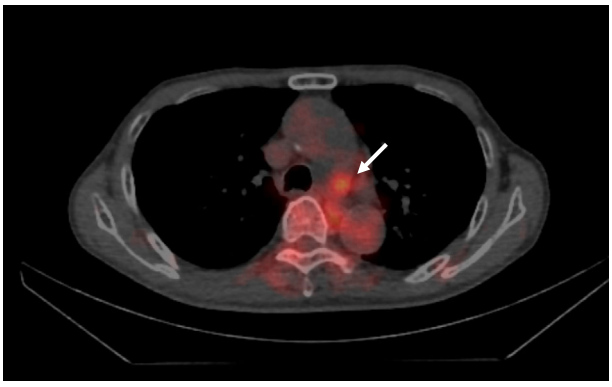

Figure 5. **Somatostatin receptor scintigraphy (SRS) localized the uptake in the left wall of the mediastinal cystic lesion (arrow).**

and synaptophysin. The Ki-67 proliferation index was less than 1%. The cells also showed some expression of SSTR5, but not SSTR2, in the cell membrane (Fig. 7). Morphological findings of carcinoma, such as vascular, capsular, or adjacent tissue invasion, were not observed.

Based on these findings, the tumor was diagnosed as an ectopic parathyroid adenoma with cystic degeneration.

Discussion

Parathyroid adenomas, the most frequent form of PHPT, usually occurs in the neck; however, in 6% of cases, they occur in ectopic locations such as the mediastinum (7). Since identification and resection of the responsible lesion is essential for achieving a radical cure, imaging studies are crucial. US, CT, MRI, and ^{99m}Tc-MIBI scintigraphy with SPECT are established preoperative localization techniques.

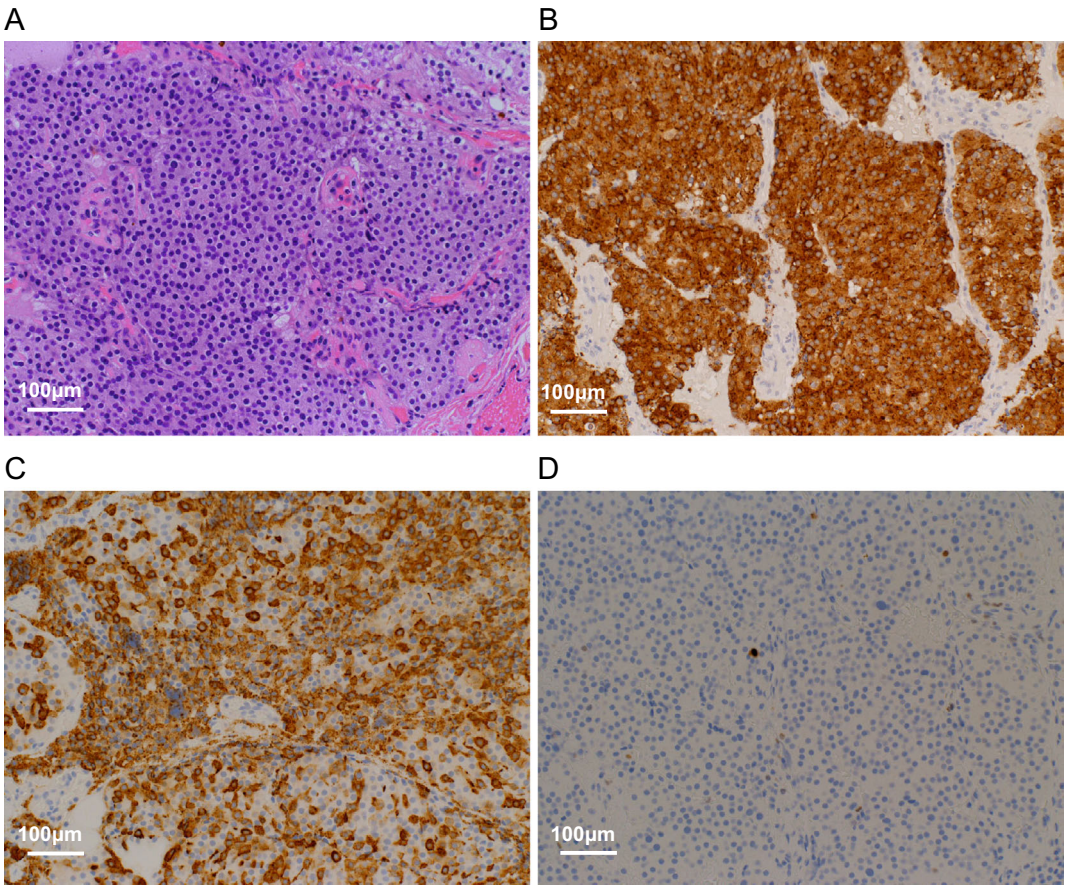

Figure 6. **The lesion was diagnosed as a parathyroid adenoma. (A) The tumor cells were parathyroid chief cells-like endocrine cells with slightly enlarged nuclei in a solid nest pattern (Hematoxylin and Eosin staining). An immunohistochemical analysis showed that the cells were positive for parathyroid hormone (PTH) (B) and chromogranin A (C). The Ki-67 proliferation index was <1% (D).**

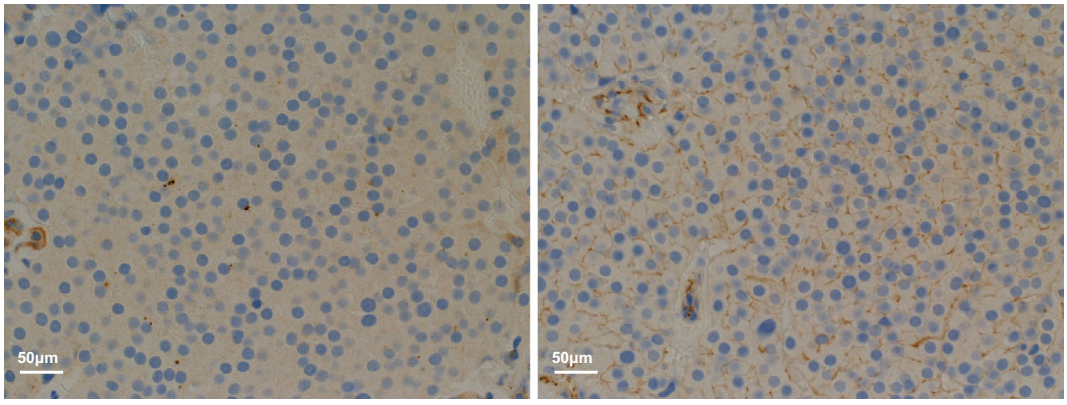

Figure 7. **SSTR5, but not SSTR2, was expressed in the tumor cell membrane.**

However, in the present case, the conventional imaging modalities only showed a bronchial cyst-like lesion in the middle mediastinum and a bone tumor-like lesion located proximal to the left femur, both of which were negative on ^{99m}Tc-MIBI scintigraphy with SPECT. Instead, using SRS, also known as ^{111}In-pentetreotide scintigraphy, we successfully identified the mediastinal lesion as a cystic parathyroid adenoma. Thus far, only a few case reports have described the use of SRS to identify cervical parathyroid adenomas (4-6). However, no report has mentioned the utility of SRS in ^{99m}Tc-MIBI-negative cases. The present case suggests the potential superiority and benefit of SRS over ^{99m}Tc-MIBI scintigraphy in some cases.

Somatostatin receptors (SSTRs) are G protein-coupled seven-transmembrane receptors that mediate the effects of the hormone somatostatin. They are often expressed in en-

docrine tumors, such as pituitary tumors and neuroendocrine tumors. Octreotide is a potent synthetic somatostatin analog, and ^{111}In-labeled pentetreotide, which is a conjugate of octreotide, accumulates in tissues expressing SSTRs. A previous study found that normal parathyroid cells express SSTRs (8). In a recent study, Storvall et al. also reported that parathyroid adenomas, atypical adenomas, and carcinomas all express SSTR subtypes 1-5 and suggested that SSTR5 may serve as a potential biomarker for malignancy (9). Furthermore, long-acting octreotide has been reported as a possible alternative treatment for PHPT due to adenomas in patients with multiple endocrine neoplasia type 1 (MEN1) (5). Based on these studies, we performed SRS, which allowed us to identify the PHPT-responsible lesion. Since octreotide binds with high affinity to SSTR2 and SSTR5 (10), we examined the SSTR2 and SSTR5 expression of the tumor. Immunohistochemistry revealed that SSTR5, but not SSTR2, was expressed in the cell membrane of the tumor cells.

^{99m}Tc-MIBI scintigraphy is an excellent diagnostic tool for the localization of ectopic PHPT (11), with a reported sensitivity of 64-90.6% and a positive predictive value of 83.5-96.0% (12). However, there are rare cases in which ^{99m}Tc-MIBI scintigraphy did not yield definite outcomes. In such cases, one alternative modality that can be used is ^{11}C-methionine positron emission tomography (PET). Several studies have reported that ^{11}C-methionine PET provides valuable additional information when conventional imaging techniques are negative or inconclusive for localizing PHPT lesions (13-16). However, because the half-life of ^{11}C is extremely short (20 min), the diagnostic agent must be synthesized just prior to testing using a cyclotron or other synthesis device. ^{18}F-fluorocholine PET has also been reported as another alternative diagnostic approach (17, 18), but its effectiveness is not yet established.

Cystic degeneration of parathyroid adenoma is seen in approximately 1-2% of patients with PHPT (19, 20). The pathogenesis of cystic adenomas is believed to result from hemorrhaging or cystic degeneration of a parathyroid adenoma (21). Gurbuz et al. reported that cystic parathyroid adenomas in the mediastinum are more likely to be functional than those in the non-mediastinum (22). Although the aspiration of cystic contents and confirmation of elevated PTH have been reported to be the most useful examinations for preoperatively diagnosing cervical cystic parathyroid adenomas (23), in the case of mediastinal lesions, aspiration is not easy to perform. Furthermore, since parathyroid cells tend to easily engraft to other organs, a serious risk of dissemination should be considered. Therefore, in our case, aspiration was not performed.

Little is known about the diagnostic accuracy of ^{99m}Tc-MIBI scintigraphy in the evaluation of cystic parathyroid adenoma. McCoy et al. reported that preoperative ^{99m}Tc-MIBI scintigraphy with SPECT was lateralized correctly in 25 of 37 (68%) patients (20), whereas Johnson et al. reported that only 4 of 14 (29%) patients were definitively identified with scintigraphy, and 3 of 14 (21%) were negative. These results suggest a lower accuracy rate of ^{99m}Tc-MIBI scintigraphy in cases of cystic parathyroid adenoma than for overall parathyroid adenoma. In such cases, SRS may be a better diagnostic tool than ^{99m}Tc-MIBI scintigraphy.

However, several studies have reported that SRS has potential utility for visualizing thymomas (24-27). Therefore, when the tumor is located in the anterior mediastinum, attention should also be paid to the possibility of thymoma.

In conclusion, we presented the first case of ^{99m}Tc-MIBI-negative cystic parathyroid adenoma in the mediastinum, which was successfully identified by SRS. SRS may be an alternative diagnostic tool when ^{99m}Tc-MIBI scintigraphy does not provide conclusive results on the localization of the parathyroid adenoma lesion. The superiority and indications for SRS are still unknown and require further study in the future.

The authors state that they have no Conflict of Interest (COI).

References

1. Bergenfelz AO, Wallin G, Jansson S, et al. Results of surgery for sporadic primary hyperparathyroidism in patients with preoperatively negative sestamibi scintigraphy and ultrasound. Langenbecks Arch Surg **396**: 83-90, 2011.
2. Sebag F, Hubbard JG, Maweja S, Misso C, Tardivet L, Henry JF. Negative preoperative localization studies are highly predictive of multiglandular disease in sporadic primary hyperparathyroidism. Surgery **134**: 1038-1041; discussion 1041-1032, 2003.
3. Sugg SL, Krzywda EA, Demeure MJ, Wilson SD. Detection of multiple gland primary hyperparathyroidism in the era of minimally invasive parathyroidectomy. Surgery **136**: 1303-1309, 2004.
4. Boulahdour H, Bertrand AM, Klingelschmitt S, et al. Parathyroid adenoma visualization on octreotide scintigraphy. Clin Nucl Med **27**: 304-305, 2002.
5. Faggiano A, Tavares LB, Tauchmanova L, et al. Effect of treatment with depot somatostatin analogue octreotide on primary hyperparathyroidism (PHP) in multiple endocrine neoplasia type 1 (MEN1) patients. Clin Endocrinol (Oxf) **69**: 756-762, 2008.
6. Karaçavuş S, Kula M, Cihan Karaca Z, et al. Octreotide uptake in parathyroid adenoma. Mol Imaging Radionucl Ther **21**: 77-79, 2012.
7. Ravipati NB, McLemore EC, Schlinkert RT, Argueta R. Anterior mediastinotomy for parathyroidectomy. Am J Surg **195**: 799-802, 2008.
8. Taniyama Y, Suzuki T, Mikami Y, Moriya T, Satomi S, Sasano H. Systemic distribution of somatostatin receptor subtypes in human: an immunohistochemical study. Endocr J **52**: 605-611, 2005.
9. Storvall S, Leijon H, Ryhänen E, et al. Somatostatin receptor expression in parathyroid neoplasms. Endocr Connect **8**: 1213-1223, 2019.
10. Colao A, Faggiano A, Pivonello R. Somatostatin analogues: treatment of pituitary and neuroendocrine tumors. Prog Brain Res **182**: 281-294, 2010.
11. Guerin C, Lowery A, Gabriel S, et al. Preoperative imaging for focused parathyroidectomy: making a good strategy even better. Eur J Endocrinol **172**: 519-526, 2015.
12. Insogna KL. Primary Hyperparathyroidism. N Engl J Med **379**: 1050-1059, 2018.
13. Beggs AD, Hain SF. Localization of parathyroid adenomas using

11C-methionine positron emission tomography. Nucl Med Commun **26**: 133-136, 2005.

14. Caldarella C, Treglia G, Isgrò MA, Giordano A. Diagnostic performance of positron emission tomography using ^{11}C-methionine in patients with suspected parathyroid adenoma: a meta-analysis. Endocrine **43**: 78-83, 2013.

15. Schalin-Jäntti C, Ryhänen E, Heiskanen I, et al. Planar scintigraphy with 123I/99mTc-sestamibi, 99mTc-sestamibi SPECT/CT, 11 C-methionine PET/CT, or selective venous sampling before reoperation of primary hyperparathyroidism? J Nucl Med **54**: 739-747, 2013.

16. Weber T, Maier-Funk C, Ohlhauser D, et al. Accurate preoperative localization of parathyroid adenomas with C-11 methionine PET/CT. Ann Surg **257**: 1124-1128, 2013.

17. Cuderman A, Senica K, Rep S, et al. ^{18}F-fluorocholine PET/CT in primary hyperparathyroidism: superior diagnostic performance to conventional scintigraphic imaging for localization of hyperfunctioning parathyroid glands. J Nucl Med **61**: 577-583, 2020.

18. Michaud L, Burgess A, Huchet V, et al. Is ^{18}F-fluorocholine-positron emission tomography/computerized tomography a new imaging tool for detecting hyperfunctioning parathyroid glands in primary or secondary hyperparathyroidism? J Clin Endocrinol Metab **99**: 4531-4536, 2014.

19. Clark OH. Parathyroid cysts. Am J Surg **135**: 395-402, 1978.

20. McCoy KL, Yim JH, Zuckerbraun BS, Ogilvie JB, Peel RL, Carty SE. Cystic parathyroid lesions: functional and nonfunctional parathyroid cysts. Arch Surg **144**: 52-56; discussion 56, 2009.

21. Som PM, Sacher M, Lanzieri CF, et al. Parenchymal cysts of the lower neck. Radiology **157**: 399-406, 1985.

22. Gurbuz AT, Peetz ME. Giant mediastinal parathyroid cyst: an unusual cause of hypercalcemic crisis--case report and review of the literature. Surgery **120**: 795-800, 1996.

23. Silverman JF, Khazanie PG, Norris HT, Fore WW. Parathyroid hormone (PTH) assay of parathyroid cysts examined by fine-needle aspiration biopsy. Am J Clin Pathol **86**: 776-780, 1986.

24. Guidoccio F, Grosso M, Maccauro M, et al. Current role of ^{111}In-DTPA-octreotide scintigraphy in diagnosis of thymic masses. Tumori **97**: 191-195, 2011.

25. Lastoria S, Vergara E, Palmieri G, et al. In vivo detection of malignant thymic masses by indium-111-DTPA-D-Phe1-octreotide scintigraphy. J Nucl Med **39**: 634-639, 1998.

26. Lin K, Nguyen BD, Ettinger DS, Chin BB. Somatostatin receptor scintigraphy and somatostatin therapy in the evaluation and treatment of malignant thymoma. Clin Nucl Med **24**: 24-28, 1999.

27. Marienhagen J, Schalke B, Aebert H, Held P, Eilles C, Bogdahn U. Somatostatin receptor scintigraphy in thymoma imaging method and clinical application. Pathol Res Pract **195**: 575-581, 1999.